

# SPEED AND FLIGHT PATH BOUNDARIES FOR WINCH LAUNCHING

By F. G. Irving

Prepared for OSTIV Sailplane Development Panel

## Summary

This paper examines the relationships between speed and flight path slope during a winch launch which define boundaries corresponding to stalling and weak link failure respectively. The speed corresponding to the intersection of these boundaries is shown to be a function of the cable angle to the horizontal for any particular glider. Simple expressions for this speed are derived, corresponding to small and large cable angles. It is recommended that the latter figure should be quoted in Flight Manuals.

## 1. Introduction.

This paper attempts to offer some explanations relating to fatal accidents in the UK in which the glider may have stalled during a winch launch. When Bill Scull, Chairman of the Training and Safety Panel of OSTIV, was looking for some technical advice, I was able to apply an existing computer program in order to define stalling and weak-link failure boundaries. This program was not initially intended for public display and was fairly user-hostile, as indicated by the sample of printout reproduced in Reference 1.

The program was subsequently refined to make it more friendly, explicit and useful. At the same time, the opportunity was taken to expand the relevant theory.

At the end of this paper, some very simple results are derived, with the intention of suggesting a safe launching speed. It was felt worthwhile to develop a fairly comprehensive and accurate theory in the first instance, both to provide an insight into the problems of winch launching and to provide a means of assessing the accuracy of the simpler results.

## 2. Assumptions.

At any instant, the glider is supposed to be in equilibrium under the influence of the aerodynamic forces, the weight and the cable force. Any acceleration, whether due to speed changes or curvature of the flight path, is therefore neglected. Intuitively, this would seem to be reasonable, except near the start of the launch.

This assumption implicitly involves another: that the balance of moments acting on the glider need not be considered. In other words, the elevator authority is such that any of the postulated equilibrium conditions can be attained. This is doubtless realistic for gliders having a markedly aft location of the winch-launching hook, together with adequate aerodynamic elevator effectiveness.

In some previous analyses of winch launching, the drag has either been neglected or a constant lift/drag ratio has been assumed (e.g., Reference 2). In fact it is not necessary to do either and the present analysis assumes a parabolic  $C_D - C_L$  polar. The effect of the drag is mostly rather small, but it does have a significant effect on the cable tension near the top of the launch. This method of accounting for the

drag probably underestimates its value at lift coefficients close to the maximum.

The method of calculating the stall boundary assumes that the maximum lift coefficient of the glider is constant and has the same value as in free flight. The overall maximum lift coefficient depends slightly on the elevator angle required to achieve it, which may not be the same as in free flight. This effect seems likely to be very small, and the stalling speed will then be proportional to the square root of the load factor,  $L/W$ . However, in unsteady conditions the value of the maximum lift coefficient may increase, leading to higher loads than those considered here.

One of the significant angles is the flight path slope, the direction of motion relative to the surrounding air. It is not the same as the glider attitude as perceived by the pilot, which is greater by the angle of attack. Nor is it the same as the flight path slope as perceived by an external observer, which is influenced by the wind.

The slope of the cable is the value at the glider. This will not be the same as the slope of a line drawn between the glider and the winch, due to the sag of the cable.

An important quantity is the ratio of the wing root bending moment during the launch to its value in free flight. Excessive values can be avoided by the use of a suitable weak link and it does not normally present a problem - but it could be critical if, in error, too strong a weak link were used. In free flight, the value of this ratio is substantially the same as the load factor. This is not the case during the winch launch, because the downward bending moment due to the wing weight is not scaled by the load

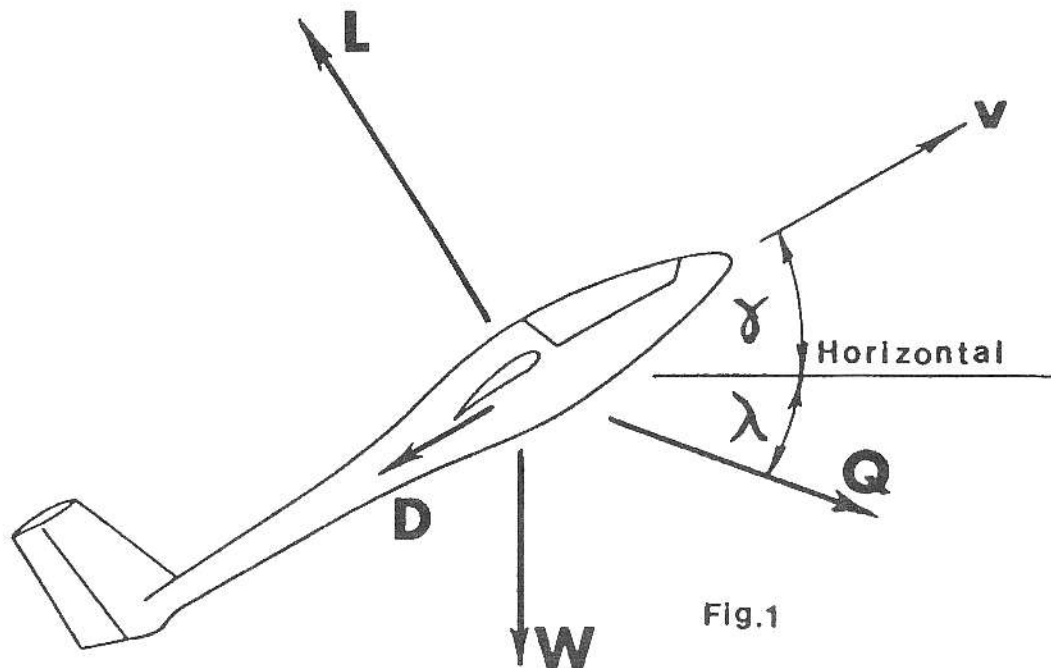


Fig.1

FIGURE 1.

factor, as is the lift. Indeed, it is diminished, as a consequence of the flight path slope. The value of the "bending moment ratio" calculated by the program WINCHER (see Figure 2) assumes that the spanwise distribution of the wing lift is elliptical and that the ratio of the wing lift to the total lift is constant. Also, details such as ignoring the weight of the wing root fittings are neglected.

Finally, the program WINCHER provides values of the "cable power", largely as a matter of general interest. This simply represents the power being supplied to the glider by the cable tension. It is worth noting that a very high proportion of this power is applied usefully to lifting the glider since the only losses are due to the glider drag. This "cable power" is obviously not the same as the power produced by the winch engine.

All the speeds are implicitly "equivalent" airspeeds, which means that the figures for cable power are only correct at sea level.

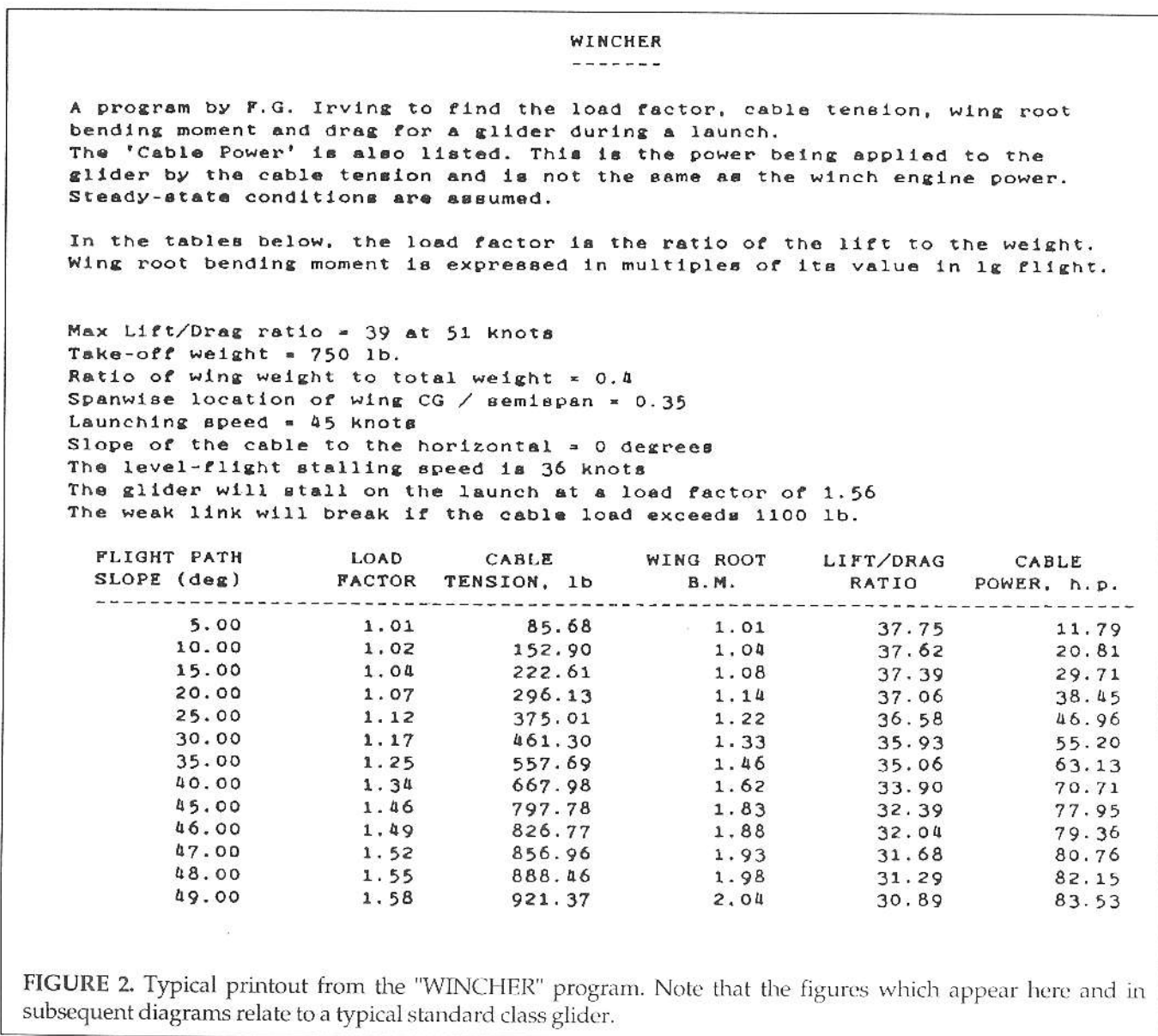
### 3. Possible Boundaries

A given glider, with the winch cable at a certain angle to the horizontal (see Figure 1), can achieve various combinations of speed and flight path slope. To some extent these will be determined by the characteristics of the winch and the way it is driven. Here, it is assumed that the winch can always enable the glider to achieve the relevant speed/flight path boundaries.

These boundaries may be determined by the following:

- (a) the stall;
- (b) breakage of the weak link;
- (c) available winch engine power;
- (d) structural loads.

Of these, (c) is unlikely to be a limitation with modern winches and, as noted above, (d) is only likely to be significant if the wrong weak link is used. This will be considered later, but the analysis below is mainly con-



cerned with (a) and (b).

#### 4. Analysis

Figure 1 shows the glider in equilibrium under the action of the forces  $L$ ,  $D$ ,  $W$  and  $Q$ . See also the list of symbols.

Resolving perpendicular to  $Q$ :

$$L \cos(\gamma + \lambda) = D \sin(\gamma + \lambda) + W \cos \lambda. \quad (1)$$

This can be rearranged so that the load factor is:

$$n = L/W = (D/W) \tan(\gamma + \lambda) + \cos \lambda / \cos(\gamma + \lambda). \quad (2)$$

Assuming a parabolic drag polar (Refs 3 & 4), the drag is given by:

$$D/W = (1/2E_{\max}) (U^2 + (n/U)^2). \quad (3)$$

Here,  $E_{\max}$  is the maximum lift/drag ratio and  $U$  is the dimensionless speed  $V/V_{md}$ . Substituting (2) in (3) gives a quadratic equation in 'n' which can be written:

$$n^2 - (2E_{\max} U^2) n / \tan(\gamma + \lambda) + U^4 + (2E_{\max} U^2 \cos \lambda) / \sin(\gamma + \lambda) = 0. \quad (4)$$

If this is expressed in the form

$$n^2 - 2Bn + C = 0,$$

then the relevant root is

$$n = B - (B^2 - C)^{1/2}. \quad (5)$$

Resolving perpendicular to the flight path:

$$Q \sin(\gamma + \lambda) + W \cos \gamma = L, \quad (6)$$

and hence the cable tension is given by:

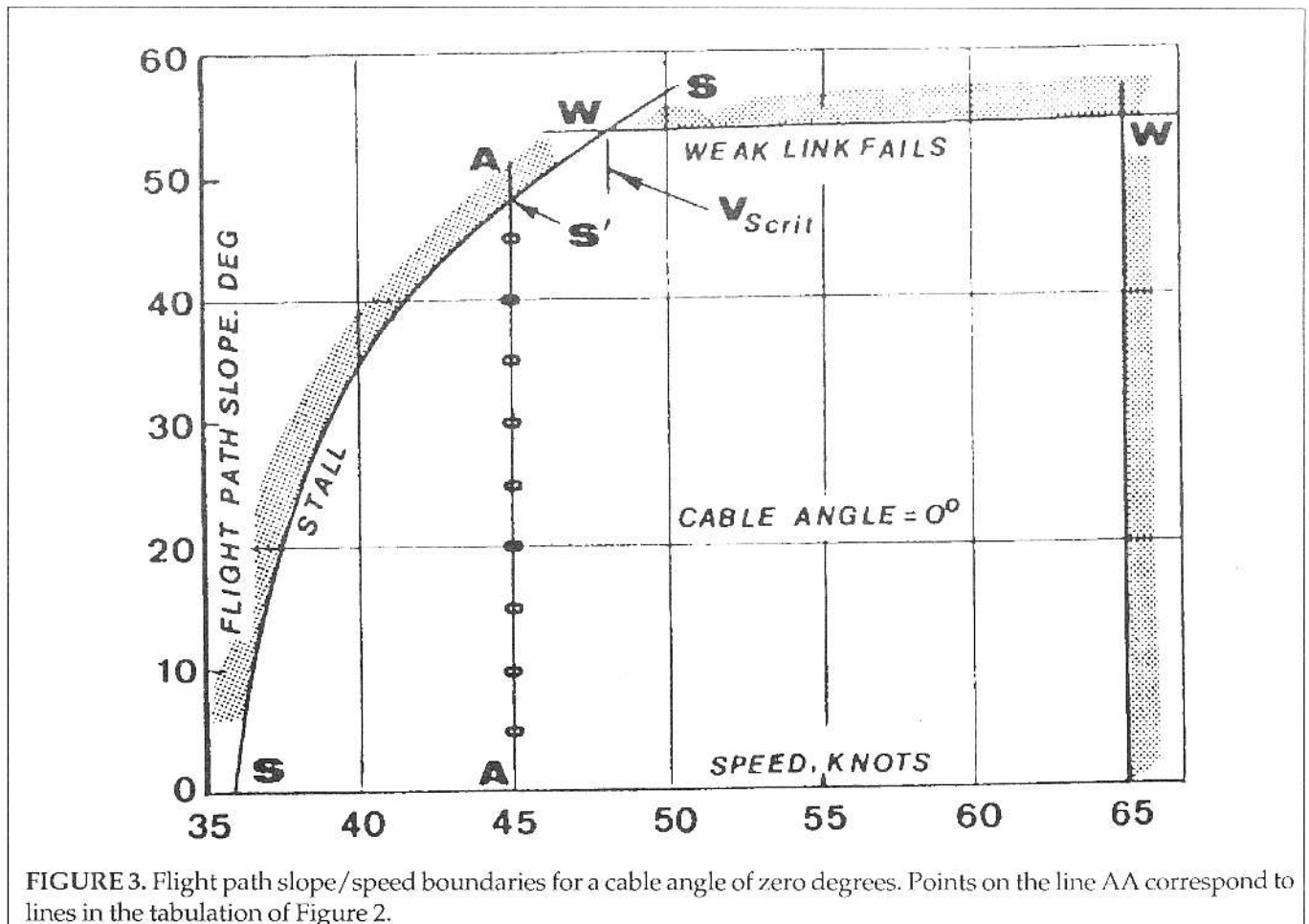
$$Q/W = (n - \cos \gamma) / \sin(\gamma + \lambda). \quad (7)$$

The lift/drag ratio may be derived from (3):

$$E = nW/D = 2E_{\max} nU^2 / (U^4 + n^2). \quad (8)$$

If the spanwise lift distribution is elliptical and the total wing lift is  $nW$ , the upward wing root bending moment will be:

$$(nW/2)(b/2)(4/3\pi). \quad (9)$$



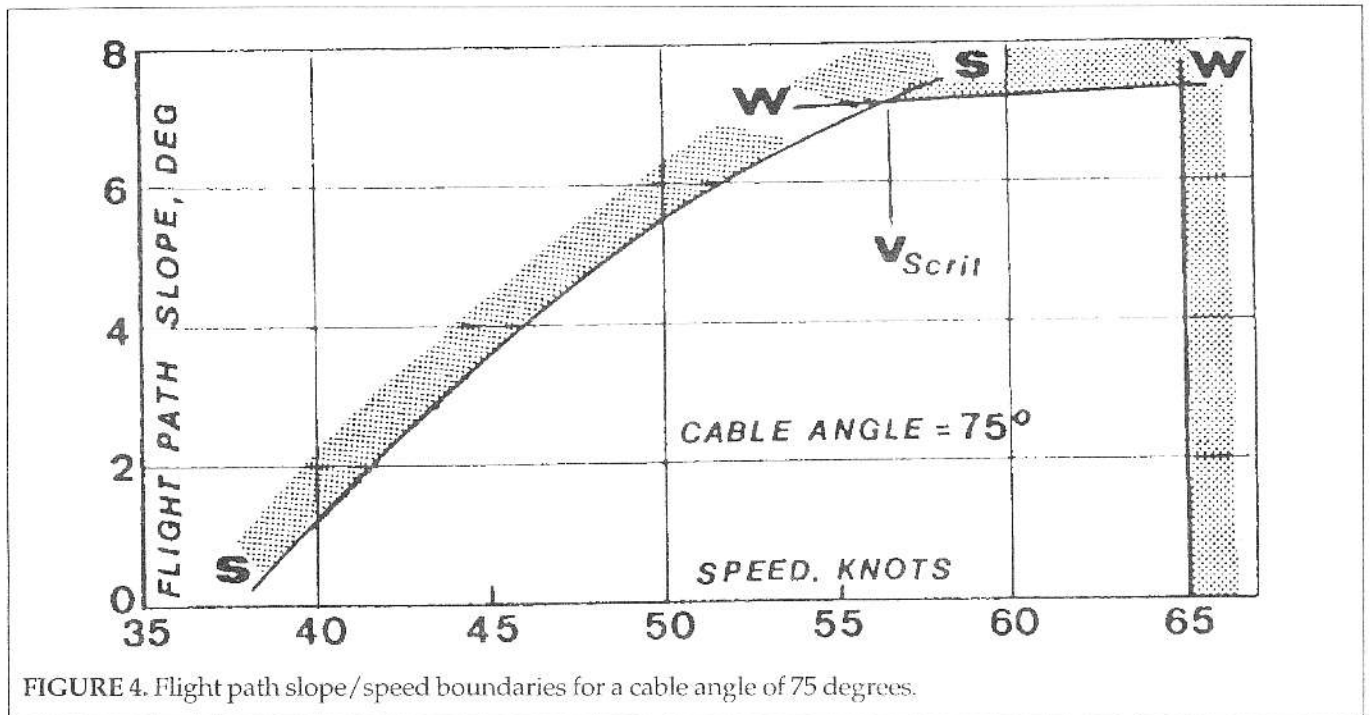


FIGURE 4. Flight path slope/speed boundaries for a cable angle of 75 degrees.

If the total wing weight is  $W_w$  and the spanwise location of the centre of gravity of one wing is  $y_G$ , then the downwards wing root bending moment will be:

$$(W_w / 2) y_G \cos \gamma. \quad (10)$$

The difference between these two quantities gives the resultant bending moment:

$$M = (Wb/3\pi) (n - W_R Y_{GR} \cos \lambda). \quad (11)$$

Here,  $W_R$  is the ratio of the wing weight to the total laden weight,  $W_w / W$ , and  $Y_{GR}$  is  $(4 / 3\pi) (2y_G / b)$ .

The ratio of the bending moment during the launch to that at  $(n = 1, \gamma = 0)$  will therefore be:

$$M_R = (n - W_R Y_{GR} \cos \gamma) / (1 - W_R Y_{GR}) \quad (12)$$

Hence, given the values of  $E_{max}$ ,  $U$ ,  $\gamma$  and  $\lambda$ , the corresponding values of  $n$  can be found from (4) and (5) and hence  $Q/W$  from (7). Knowing the speed for best glide angle,  $V_{md}$ , and the weight  $W$ , the actual speed  $V$  and the cable tension  $Q$  can be found.

The above equations involve only dimensionless quantities such as the load factor or ratios such as  $Q/W$ . The convenience of this approach is that the equations are of general applicability and only require the knowledge of a few straightforward quantities such as the maximum lift/drag ratio and the corresponding speed to obtain results for a specific glider.

## 5. Application.

A computer program based on the above analysis is

easily devised. One possibility is to produce an output such as that shown in Figure 2. The input consists of the characteristics of the glider, the cable angle and the launch speed. A series of values of the flight path slope are then chosen. The output then relates to a series of points on a line such as AA in Figure 3. The glider chosen for this example is approximately an ASW-19.

Boundaries such as the stalling boundary SS and the weak link failure boundary WW may be deduced by inspecting the output and, if necessary, making the appropriate interpolations.

For example, if the stalling speed in steady 1g free flight is  $V_{st}$  and the launch speed is  $V$ , then the glider will stall at a load factor  $n_s$  where

$$n_s = (V / V_{st})^2 \quad (13)$$

In Fig.2, the speed is 45 knots,  $n_s$  is 1.56 and therefore corresponds to a flight path slope of about 48 degrees, or point S' in Figure 3. The corresponding cable tension is 888 lb. so, given a weak link of 500 kp (1100 lb.), the stall is attained before the weak link breaks.

By proceeding in this fashion, for a series of different speeds, the stalling boundary SS can be established.

Similarly, by noting the combinations of speed and flight path slope which produce a cable tension equal to the weak link strength (taken as 1100 lb. in this example), the boundary WW can be defined.

When the speed is 48 knots,  $n_s$  is 1.77 and is attained at a flight path slope of just under 54 degrees. The corresponding cable load is 1100 lb, so the boundaries intersect here. At higher speeds, the weak link will break before the stall occurs.

Figure 3 assumes a cable angle of zero, implying that the

glider is only just clear of the ground. Obviously, no pilot in his or her right mind would wish to achieve a flight path slope of 54 degrees in such circumstances. This case is only inserted to display an extreme theoretical condition.

It will be noted that the boundary WW corresponds very nearly to a constant flight path slope (about 54 degrees in Figure 3). The variations in lift/drag ratio are responsible for the departure from constancy.

In Figure 3, flight is possible anywhere within the area bounded by SS, WW,  $\gamma = 0$  and  $V = 65$  knots (the maximum permitted launch speed in this example). If required, the diagram could be elaborated by inserting lines of constant load factor or wing root bending moment ratio.

A similar diagram can be drawn for other cable angles. Another extreme case corresponds to  $\lambda = 75$  degrees, the greatest angle considered in airworthiness requirements such as JAR 22, leading to boundaries as shown in Figure 4. Note the greatly expanded vertical scale compared with that of Figure 3. The significant features are that the stalling speed can be as high as 56 knots, about 55% higher than the free flight lg value, and that small flight path slopes lead to large increments in stalling speed.

#### 6. The stalling boundary in more detail.

If the stalling speed at any point on the stalling boundary

is  $V_s$  and  $U_s$  is the corresponding dimensionless quantity then, on the boundary,  $U$  in (4) becomes  $U_s$  and, from (13),  $n$  becomes  $(U_s/U_{st})^2$ . After some rearrangement, (4) leads to:

$$U_s = (2E_{\max} \cos \lambda) U_{st} / 2E_{\max} U_{st} \cos(\gamma + \lambda) - (1 + U_{st} \sin(\gamma + \lambda)) \quad (14)$$

This gives  $U_s$  and hence  $V_s$  as an explicit function of the cable angle and flight path slope, given the properties of the glider. Again, the above equations enable the corresponding values of the cable tension to be found. Hence the maximum stalling speed for a given flight path angle,  $V_{scrit}$ , when the cable tension corresponds to weak link strength, can also be found. Figure 5 shows these stalling boundaries for various cable angles, together with the locus of  $V_{scrit}$  as a function of cable angle.

#### 7. Approximations.

Expressions such as (14) are fairly complicated and, for practical purposes, something simpler would be desirable. The obvious simplification is to neglect the drag, on the grounds that this is a small force compared with others acting on the glider. The expression for the stalling speed, corresponding to (14), then becomes:

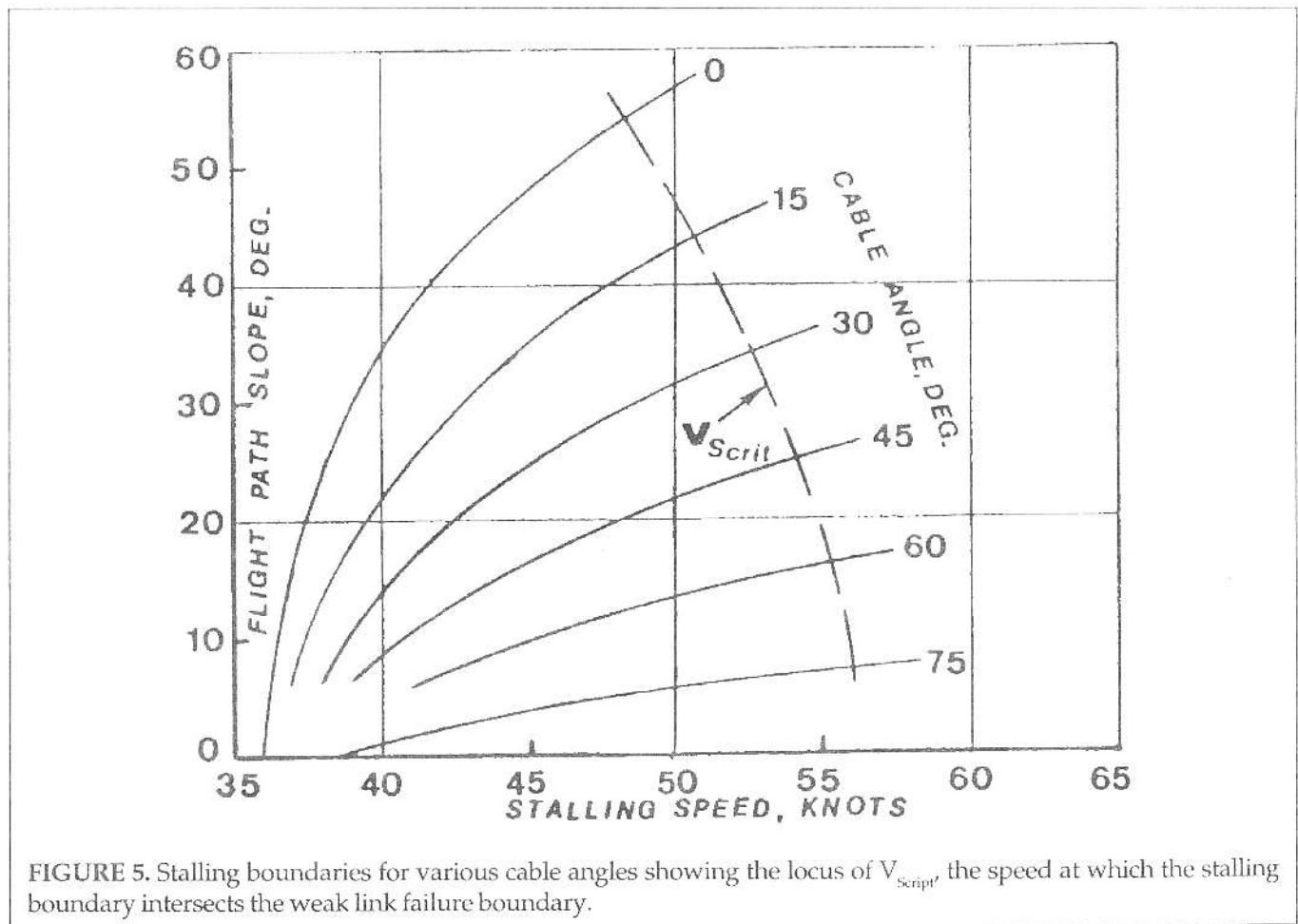


FIGURE 5. Stalling boundaries for various cable angles showing the locus of  $V_{scrit}$ , the speed at which the stalling boundary intersects the weak link failure boundary.

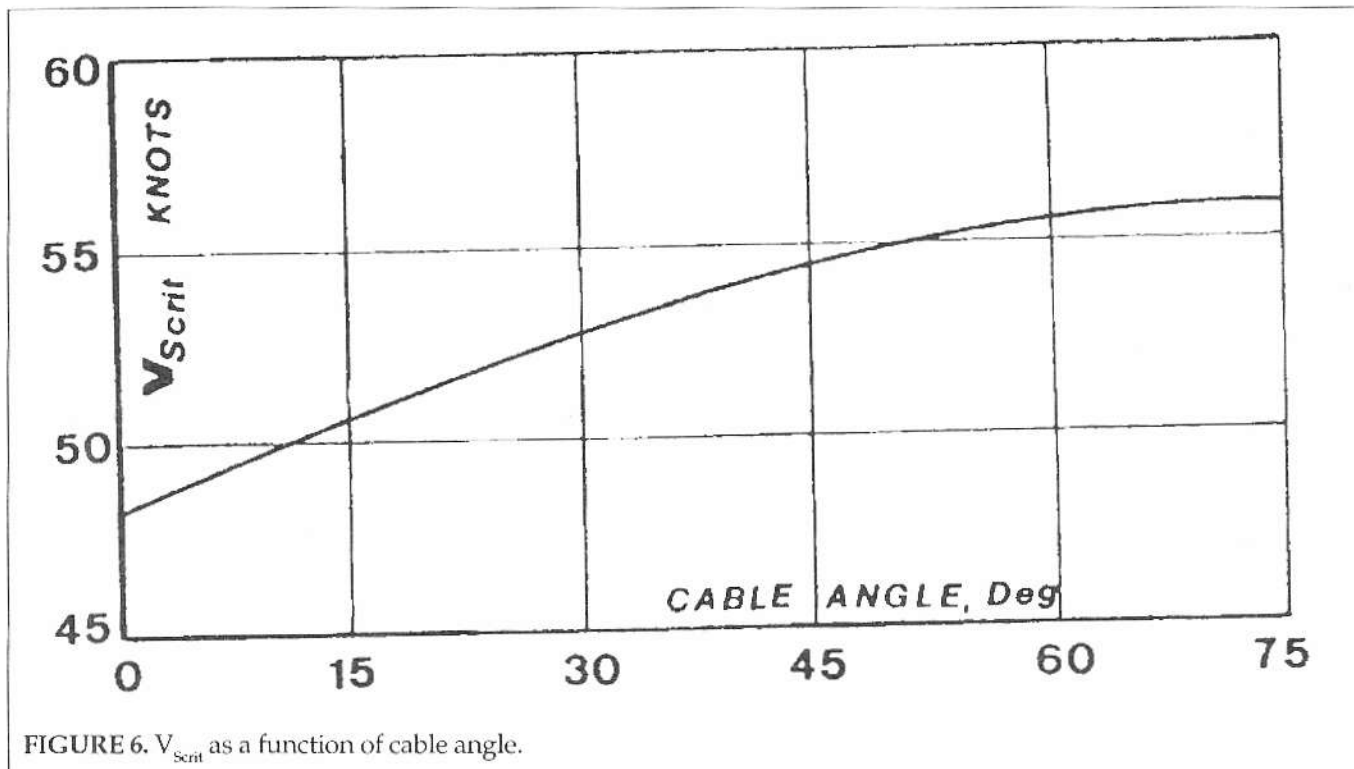


FIGURE 6.  $V_{Scrit}$  as a function of cable angle.

$$V_s = V_{st} (\cos \lambda / \cos (\gamma + \lambda))^{1/2}. \quad (15)$$

For given values of  $\lambda$  and  $\gamma$ , this expression underestimates the stalling speed since removal of the drag decreases the required cable tension and hence decreases the load factor. However, the greatest interest attaches to the values of  $V_{Scrit}$  at extreme cable angles. If the drag is again neglected and if the weak link strength is  $Q_{max}$ , then, from (2) and (7), with  $\lambda = 0$ :

$$n = \sec \gamma \quad (16)$$

$$Q/W = \tan \gamma, \quad (17)$$

and on the stalling boundary,

$$(VS/V_{st})^2 = n = \sec \gamma. \quad (18)$$

Hence, from (17) and (18), when  $Q = Q_{max}$ ,

$$V_{Scrit} = V_{st} (1 + (Q_{max}/W)^2)^{1/4}. \quad (19)$$

Taking the figures for the Standard Class glider considered above, with  $Q_{max} = 1100$  lb,  $V_{Scrit}$  from (19) is 48 knots, which is almost exactly correct. (The corresponding flight path slope turns out to be 56 degrees, or about 2 degrees more than the "accurate" value. In effect, the greater flight path slope compensates for the neglect of the drag).

If  $\lambda$  is large and  $\gamma$  is small, then  $\sin (\lambda + \gamma) \rightarrow 1$  and  $\cos \gamma \rightarrow 1$ , so

$$Q/W = n - 1, \text{ approx.} \quad (20)$$

Hence, at  $V_{Scrit}$  from (18) and (20),

$$V_{Scrit} = V_{st} (1 + (Q_{max}/W))^{1/2} \quad (21)$$

For the present example,  $V_{Scrit}$  becomes 56.5 knots which, again, is almost exactly the same as the "accurate" value. The load factor from (20) is 2.47, also very close to the "accurate" value. A detailed calculation shows that neglecting the drag produces a flight path slope about 1.5 degrees greater than the "accurate" value at weak link failure. Once more, the increase in flight path slope compensates for the absence of drag.

### 8. Effect of ballast

At  $W = 750$  lb and  $\lambda = 0$ ,  $V_{Scrit}$  is 48 knots in the above example. If the weight is increased to 900 lb. by water ballast,  $Q_{max}/W$  decreases from 1.47 to 1.22 but  $V_{st}$  increases from 36 to 39.4 knots.  $V_{Scrit}$  then becomes 49.5 knots, a small increase.

At large values of  $\lambda$ ,  $V_{Scrit}$  increases from 56.5 to 58.7 knots.

### 9. The consequences of stalling

Recent accidents have shown that the consequences of stalling just after the start of a launch may be fatal. In particular, a wing drop may lead to something not unlike the beginning of a flick roll if the winch continues to pull.

Stalling, and possible spinning, towards the top of a launch might be thought less dangerous: given a reasonable height of launch, there should be sufficient height

available for recovery. However, another recent accident in the UK indicated otherwise.

In general, breaking the weak link would seem to be safer than stalling. There is no reason for a wing to drop or for loss of control and recovery consists of a reasonably prompt pushover. If the start of the pushover occurs at a certain speed and height then, neglecting the drag, the same speed will be attained when the initial height is again reached. The effect of drag on such a manoeuvre, if performed reasonably briskly, is quite small. This of course, assumes that there is sufficient elevator authority to perform the manoeuvre satisfactorily. Even so, it would seem extremely imprudent to pull up so steeply just after the start of a launch that the weak link breaks, as in Figure 3, at a flight path slope of 54 degrees and a speed of perhaps 50 knots.

The above suggests that it is desirable to be flying at a speed greater than  $V_{scrit}$  at the beginning of the launch and preferably throughout the launch. Attempting to climb too steeply will then result in failure of the weak link and not in a stall. Some Flight Manuals already give some advice on these lines. For example, that of the Grob G-103C states that the normal launching speed is approximately 62 knots. This agrees very closely with the value given by (21).

## 10. Effect of weak link strength

Increasing the weak link strength, other things being equal, will move the WW boundary upwards in diagrams such as Figure 3. It will be possible to stall the glider at higher speeds and steeper flight path slopes and, on the weak link failure boundary, the load factor and wing root bending moment ratio will be increased.

For example, if the Standard Class glider of the above calculations were launched in error on a 2200 lb. weak link then, with a cable angle of 75 degrees, a load factor of 3.9 could be achieved if the glider were flying at 71 knots (6 knots above the maximum winch launch speed). The wing root bending moment ratio would be 5.34, corresponding to conditions slightly outside the manoeuvring envelope and possibly leading to damage. This situation assumes that the hook and the structure to which it was attached did not fail first.

Moral: always ensure that the correct weak link is used and respect the winching speed limitation.

## 11. Conclusions

(i) For a given glider performing a winch launch with a given angle of the launch cable to the horizontal (at the glider) it is possible to derive relationships between the speed and the flight path slope corresponding to the glider stalling or the weak link breaking.

(ii) It is thus possible to define boundaries within which operation is possible, consisting of the above stalling and weak link failure boundaries, together

with the conditions that the flight path slope should be positive and the maximum permitted winch launch speed should not be exceeded.

(iii) There is a speed corresponding to the intersection of the boundaries mentioned in (i), denoted by  $V_{scrit}$ . At lower speeds, attempts to climb steeply will cause the glider to stall before the weak link breaks. At higher speeds, the converse situation will apply.

(iv) Expressions for  $V_{scrit}$  are as follows:

At small cable angles,

$$V_{scrit} = V_{st} (1 + (Q_{max}/W)^2)^{1/4} \quad (19)$$

whilst at large angles,

$$V_{scrit} = V_{st} (1 + (Q_{max}/W))^{1/2} \quad (21).$$

Although various approximations have been made in deriving these expressions, they are quite accurate.

## 12. Recommendations

If it is accepted that breaking the weak link is likely to be less hazardous than stalling the glider, then it is desirable that the speed should exceed  $V_{scrit}$  at all times during the launch. Since  $V_{scrit}$  is a function of cable angle, some simplified rule is required for practical application. The highest value of  $V_{scrit}$  is given by equation (21), so the simplest rule is that the speed should not normally be less than this value. (Launching at a lower speed is feasible provided that the pilot does not try to climb too steeply). For a typical Standard Class glider, the relevant speed would be about 56 knots. It is proposed that the figure calculated from equation (21) should be quoted in the Flight Manual.

Throughout this paper, it has been assumed that the weak link will break when the load in the cable reaches the rated ultimate strength of the weak link,  $Q_{nom}$ . This is consistent with the consideration of steady-state conditions, which will implicitly exclude surge loads.

However, for stressing purposes, OSTIVAS section 3.62 requires cable loads up to  $1.2Q_{nom}$  to be considered. The factor of 1.2 is intended to deal with suddenly-applied loads together with a weak link which is 20% over-strength as a consequence of manufacturing tolerances.

If it is desired to consider the effects of the higher cable loads on the boundaries,  $Q_{max}$  in the paper simply becomes  $1.2Q_{nom}$  in equations (19) and (21), for example. Using the figures for the Standard Class glider of the paper, increasing the weak link strength from 1100 lb. to 1320 lb. increases  $V_{scrit}$  by 3 knots at low cable angles and 3.3 knots at large angles. In the latter case it becomes no less than 59.8 knots (60 in round figures). At a cable angle of 75° and a speed of 65 knots, the wing root bending moment ratio at weak link failure increases from 3.16 to 3.60.



## SYMBOLS

B	A coefficient in equation (5)
b	Wing span
C	A coefficient in equation (5)
$C_D$	Drag coefficient, $D/0.5 \rho V^2 S$
$C_L$	Lift coefficient, $L/0.5 \rho V^2 S$
D	Drag
E	Lift/drag ratio
$E_{max}$	Maximum lift/drag ratio
L	Lift
M	Wing root bending moment
$M_R$	Ratio of the wing root bending moment to that in free flight at $n=1$ .
n	Load factor, $L/W$
$n_s$	Load factor at the stall
Q	Cable tension
$Q_{max}$	Maximum cable tension when the weak link fails
S	Wing area
U	Dimensionless speed, $V/V_{md}$
$U_s$	Dimensionless stalling speed, $V_s/V_{md}$
$U_{S1}$	Dimensionless stalling speed in free flight at $n = 1$ , i.e. $V_{S1}/V_{md}$
V	Airspeed
$V_{md}$	Minimum drag speed
$V_s$	Stalling speed
$V_{S1}$	Stalling speed in free flight at $n = 1$
$V_{Scnt}$	Speed at the intersection of the stalling and weak link failure boundaries
W	Total weight of the glider
$W_w$	Total wing weight
$W_R$	$W_w/W$
YG	Spanwise location of the centre of gravity of one wing
$Y_{GR}$	$(4/3\pi) (2y_G/b)$
$\gamma$	Flight path slope, positive upwards
$\lambda$	Slope of the towing cable at the glider relative to the horizontal, positive downwards
$\rho$	Air density

Note that all speeds are "equivalent", i.e., V is strictly the true airspeed multiplied by  $(\rho/\rho_0)^{1/2}$ , where  $\rho_0$  is the standard sea level air density.

### References

1. Scull, W.G. "Accidental Spins off Winch Launches". *Sailplane & Gliding*, Dec 1991/Jan 1992.
2. Gibson, J. "A Look at Winch Launching". *Sailplane*

& *Gliding*, Aug/Sept 1985.

3. Welch, A. & L., and Irving, F. G. "New Soaring Pilot". John Murray, 1977. Appendix 7.
4. Miele, A. "Flight Mechanics, Vol. 1, Theory of Flight Paths", Pergamon, 1962, p.151-152.